Review in Advance first posted online on May 4, 2017. (Changes may still occur before final publication online and in print.)

Circuits and Mechanisms for Surround Modulation in Visual Cortex

Alessandra Angelucci,[1] Maryam Bijanzadeh,[1] Lauri Nurminen,[1] Frederick Federer,[1] Sam Merlin,[1,*] and Paul C. Bressloff[2]

[1]Department of Ophthalmology and Visual Science, Moran Eye Institute, University of Utah, Salt Lake City, Utah 84132; email: alessandra.angelucci@hsc.utah.edu, ma.bijanzadeh@gmail.com, larsnurminen@gmail.com, sammerlin7@gmail.com, freddieneuron@gmail.com

[2]Department of Mathematics, University of Utah, Salt Lake City, Utah 84132; email: bressloff@math.utah.edu

Annu. Rev. Neurosci. 2017. 40:425–51

The *Annual Review of Neuroscience* is online at neuro.annualreviews.org

https://doi.org/10.1146/annurev-neuro-072116-031418

*Current address: Medical Science, School of Science and Health, Western Sydney University, Campbelltown, New South Wales 2560, Australia

Keywords

striate cortex, primary visual cortex, extrastriate cortex, feedback, horizontal connection, recurrent circuits

Abstract

Surround modulation (SM) is a fundamental property of sensory neurons in many species and sensory modalities. SM is the ability of stimuli in the surround of a neuron's receptive field (RF) to modulate (typically suppress) the neuron's response to stimuli simultaneously presented inside the RF, a property thought to underlie optimal coding of sensory information and important perceptual functions. Understanding the circuit and mechanisms for SM can reveal fundamental principles of computations in sensory cortices, from mouse to human. Current debate is centered over whether feedforward or intracortical circuits generate SM, and whether this results from increased inhibition or reduced excitation. Here we present a working hypothesis, based on theoretical and experimental evidence, that SM results from feedforward, horizontal, and feedback interactions with local recurrent connections, via synaptic mechanisms involving both increased inhibition and reduced recurrent excitation. In particular, strong and balanced recurrent excitatory and inhibitory circuits play a crucial role in the computation of SM.

Contents

1. INTRODUCTION

1.1. Surround Modulation as a Canonical Computation

Natural visual images consist of many spatially distributed stimuli that activate the entire retina at once. Yet historically, visual neurophysiologists have characterized the responses of single neurons to isolated local stimuli. This has led to the classical definition of a visual neuron's receptive field (RF) as the visual field region where presentation of stimuli of optimal parameters for the neuron evokes a spiking response (Hubel & Wiesel 1959). However, it was later discovered that a visual stimulus extending beyond a neuron's RF, or simultaneous presentation of stimuli inside and outside the RF, modulate the neuron's response to stimuli inside the RF. This property, termed surround modulation (SM), is always active during natural vision and, therefore, is an integral part of visual information processing, because natural visual stimuli do activate neurons not in isolation but within the context of other stimuli.

SM is a fundamental property of visual neurons that has been described in many species (mouse, cat, monkey, and human) at many levels of the visual system, including the retina (McIlwain 1964, Solomon et al. 2006), superior colliculus (Sterling & Wickelgren 1969, Goldberg & Wurtz 1972), lateral geniculate nucleus (LGN) (Levick et al. 1972, Marrocco et al. 1982, Solomon et al. 2002, Bonin et al. 2005, Sceniak et al. 2006, Alitto & Usrey 2008), pulvinar (Chalupa et al. 1983, Berman & Wurtz 2011), striate or primary visual cortex (V1) (Hubel & Wiesel 1965, Blakemore & Tobin 1972, Maffei & Fiorentini 1976, Gilbert 1977, Nelson & Frost 1978, Sceniak et al. 2001, Cavanaugh et al. 2002a, Van den Bergh et al. 2010, Angelucci & Shushruth 2013), and extrastriate cortex (Allman et al. 1985, Desimone & Schein 1987, Born & Bradley 2005). Although particularly well characterized in the visual cortex, SM has been described in all sensory systems, including auditory (Knudsen & Konishi 1978, Sutter et al. 1999), somatosensory (Vega-Bermudez & Johnson 1999, Sachdev et al. 2012), and olfactory systems (Olsen & Wilson 2008), suggesting it plays a fundamental role in sensory processing.

1.2. Function of Surround Modulation

A main property of SM is that dissimilar stimuli (e.g., stimuli of different orientation) inside and outside a neuron's RF generally evoke stronger responses from the neuron, compared to similar stimuli. This results in an enhancement of neuronal responses in regions of discontinuities in a sensory stimulus—for example, orientation, motion, or texture discontinuities. This observation led to the initial suggestion that SM plays a role in visual saliency and pop-out (Knierim & Van Essen 1992), perception of object boundaries (Nothdurft et al. 2000), and figure-ground segregation (Lamme 1995). However, other investigators observed facilitatory surround effects when small, iso-oriented, and collinearly aligned line segments were presented simultaneously inside and outside a neuron's RF. This observation led to the suggestion that SM may also serve perceptual contour integration (Kapadia et al. 1995, Polat et al. 1998, Field et al. 2013).

The role of SM has also been considered within a theoretical framework of visual information processing and efficient coding of natural stimuli (Barlow 1961, 1972). According to these theories, natural images contain strong spatial and temporal correlations [i.e., highly redundant information (Field 1987)], and SM would serve to reduce these redundancies in neuronal responses and to increase response sparseness. A code with less redundancy and increased sparseness is more efficient, because each spike transmits more information about a stimulus (Olshausen & Field 1996, Schwartz & Simoncelli 2001, Vinje & Gallant 2002). Reduction in pairwise neuronal correlations and increased sparseness by SM have, indeed, been demonstrated experimentally (Vinje & Gallant 2000, Haider et al. 2010, Pecka et al. 2014). Perceptual and efficient-coding theories of SM are not mutually exclusive, as, for example, in V1 redundancy reduction by SM can lead to extraction of object boundaries (Nurminen & Angelucci 2014) (see Section 2.2 below).

Figure-ground segregation: perceptual ability to separate foreground (figure) from background in visual images based on grouping and segmenting similar elements from dissimilar elements

Contour integration: perceptual ability to group and segregate into a contour collinear line segments from a background of randomly oriented segments

Sparseness: measure of the shape of a neuron's firing rate distribution in response to a fixed set of stimuli; neurons with high sparseness respond to fewer stimuli and therefore are highly selective

1.3. What Are the Circuits and Mechanisms for Surround Modulation?

A mechanistic understanding of SM requires identification of the neural circuits and synaptic mechanisms that generate it and has the potential to reveal fundamental principles of computations in sensory systems. There is lack of consensus about which pathways and mechanisms generate SM. Geniculocortical feedforward connections, long-range horizontal connections within a cortical area, and top-down feedback connections between cortical areas have all been implicated. Moreover, it is still debated whether the suppressive influence of SM (surround suppression) is mediated by increased inhibition or reduced excitation (Sachdev et al. 2012, Wolf et al. 2014, Miller 2016). In this review, we present our working hypothesis, based on both theoretical and experimental studies, that feedforward, horizontal, and feedback connections all contribute to SM, but operate at different spatiotemporal scales and within different stimulus attributes, through a common mechanism involving both increased inhibition and reduced excitation, via interactions with local inhibitory neurons and local recurrent networks. We focus on area V1, where SM has been investigated most extensively.

2. PROPERTIES OF SURROUND MODULATION

2.1. Spatiotemporal and Stimulus-Tuning Properties of Surround Modulation

A good model of SM must account for its main properties. These have been characterized in many species, but more extensively in cat and primate V1, typically using circular grating patches of increasing radius (**Figure 1**), or grating patches confined to the RF surrounded by annular gratings, and varying systematically the grating parameters. These studies are reviewed in Angelucci & Shushruth (2013) and thus are summarized only briefly here.

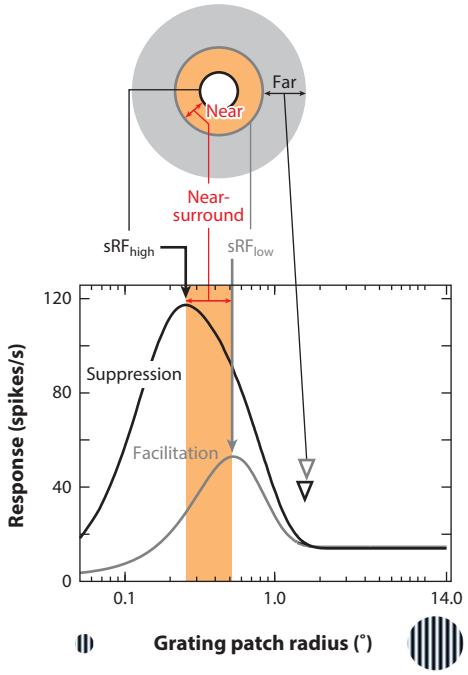

Figure 1

Spatial summation and SM in V1. Response of a cell in macaque V1 to high-contrast (*black curve*) and low-contrast (*gray curve*) grating patches of increasing radius. The cell's response increases up to a peak, corresponding to the size of the sRF at high (sRF$_{high}$, *thick black arrow*) or low (sRF$_{low}$, *thick gray arrow*) contrast, and then is suppressed as the stimulus extends into the RF surround. At low contrast, the peak of the size-tuning curve is shifted to the right relative to the high contrast peak. The near-surround is the region between the sRF$_{high}$ and sRF$_{low}$ (*orange shading*). Stimulation of this region causes suppression at high contrast but facilitation at low contrast. The far-surround is the region beyond the near-surround (*gray annulus*). Far-SM shows similar contrast dependence to near-SM. Arrowheads indicate the surround radius. The diagram at the top is a schematic representation of the different components of the sRF and surround. Figure modified from Shushruth et al. (2009). Abbreviations: SM, surround modulation; sRF, summation receptive field.

SM in V1 shows the five main properties described below.

1. SM is spatially extensive. In primates, modulatory effects from the surround (both facilitatory and suppressive) can be evoked 12.5° away (or more) from a neuron's RF center, but modulation strength decreases with increasing distance from the RF (Sceniak et al. 2001, Cavanaugh et al. 2002a, Levitt & Lund 2002, Shushruth et al. 2009).
2. SM is tuned to specific stimulus parameters. Strongest suppression is induced by stimuli in the RF and surround of the same orientation, spatial frequency, drift direction, and speed, and weaker suppression or facilitation is induced by stimuli of orthogonal parameters (e.g., orthogonally oriented stimuli or stimuli drifting in opposite directions) (DeAngelis et al. 1994, Li & Li 1994, Sengpiel et al. 1997, Walker et al. 1999, Cavanaugh et al. 2002a, Müller et al. 2003, Webb et al. 2005, Henry et al. 2013, Self et al. 2014). Importantly, the orientation tuning of SM is independent of the orientation preference of the recorded neurons: Strongest suppression occurs for iso-oriented stimuli in the RF and surround, even if the stimulus in the RF is not at the neuron's preferred orientation (Sillito et al. 1995, Cavanaugh et al.

2002b, Shushruth et al. 2012), provided that such a stimulus evokes a response from the neuron when presented in the RF alone (Shushruth et al. 2012).

3. SM is contrast dependent. Surround stimulation evokes suppression when the stimulus in the RF is of high contrast (DeAngelis et al. 1994, Levitt & Lund 1997, Sengpiel et al. 1997, Walker et al. 2000, Sceniak et al. 2001, Cavanaugh et al. 2002a, Nienborg et al. 2013), but can be facilitatory when it is of low contrast (**Figure 1**) (Sengpiel et al. 1997, Sceniak et al. 1999, Ichida et al. 2007). Moreover, at low contrast, SM is spatially more extensive (Shushruth et al. 2009) and less orientation selective (Cavanaugh et al. 2002b, Hashemi-Nezhad & Lyon 2012), has delayed onset (Henry et al. 2013), and exerts weaker suppression (Cavanaugh et al. 2002a, Sadakane et al. 2006, Schwabe et al. 2010) than at high contrast. More generally, the strength of activation of both the RF and surround is the factor that most affects the sign and strength of SM: When the RF is strongly activated (e.g., by a high-contrast stimulus of optimal orientation and size), weak or strong surround stimulation causes suppression; however, when the RF is weakly activated (e.g., by a stimulus of low contrast or of suboptimal orientation or size), weak surround stimulation (e.g., by a small, high- or low-contrast stimulus) can evoke facilitation (Polat et al. 1998, Chen et al. 2001, Ichida et al. 2007, Shushruth et al. 2012), whereas strong surround stimulation (e.g., by a large, high- or low-contrast stimulus) evokes suppression.
4. SM develops rapidly and dynamically in time. The earliest component of suppression is independent of stimulus orientation in the surround (untuned suppression), and in many V1 neurons can occur as fast as the onset of the RF response (0-ms delay) (Müller et al. 2003, Henry et al. 2013); instead, the later component of suppression is stronger for iso-oriented than for orthogonally oriented stimuli in the RF and surround (tuned suppression) and is delayed by about 10–30 ms relative to the onset of visually evoked RF responses (Bair et al. 2003) and of untuned suppression (Henry et al. 2013).
5. The properties of SM differ across cortical layers, suggesting different circuits and mechanisms generating SM in different layers. Specifically, in layer 4C, which receives inputs from the LGN and lacks long-range intracortical connections, surround fields are smaller than in other layers, and SM is weaker and untuned for orientation. Moreover, SM is stronger and more sharply orientation-tuned in supragranular layers (4B and above) compared to infragranular layers (Sceniak et al. 2001; Ichida et al. 2007; Shushruth et al. 2009, 2013; Henry et al. 2013).

2.2. Near- and Far-Surround Modulation

A consequence of the contrast dependence of SM is that RF size measured at low stimulus contrast is larger than when measured at high contrast (Sengpiel et al. 1997, Sceniak et al. 1999). This is evident in **Figure 1** as a shift in the peak of the low-contrast size-tuning curve toward larger stimuli, compared to the peak of the high-contrast size-tuning curve. We term the RF size based on these measurements the summation RF at high (sRF_{high}) or low (sRF_{low}) contrast to distinguish it from different measures of RF size (as discussed in Angelucci & Bressloff 2006), which can be contrast invariant (Song & Li 2008). As indicated in **Figure 1**, stimulation of the region between the sRF_{high} and sRF_{low} causes suppression at high contrast but facilitation at low contrast. We term this region the near-surround and the region beyond it the far-surround.

Experimental evidence suggests that these two surround regions have different spatiotemporal and stimulus-tuning properties, are generated by different circuits, and likely serve different perceptual functions (Angelucci & Bressloff 2006, Nurminen & Angelucci 2014). Specifically, near-SM in V1 cells is more strongly suppressive (Shushruth et al. 2009) and more sharply

orientation-tuned than far-SM (Hashemi-Nezhad & Lyon 2012, Shushruth et al. 2013), similar to the orientation tuning of near- and far-SM of perceived contrast in human observers (Shushruth et al. 2013).

We (Shushruth et al. 2013, Nurminen & Angelucci 2014) have suggested previously that the different tuning of near- and far-SM may reflect a statistical bias in the distribution of oriented elements in natural images. In natural images, there is a statistical relation between the orientation of edges and distance between edges, such that nearby edges are more likely than distant edges to belong to the same object contour if they are of similar orientation (Geisler et al. 2001). Thus, near-surround suppression is stronger for similarly oriented nearby edges that occur with higher probability in natural images, and less suppressive or facilitatory for nearby edges of dissimilar orientation that occur with less probability. In line with current theories of efficient coding (see Section 1.2 above), this relationship suggests that near-SM increases the sparseness of the neural code in V1 (Vinje & Gallant 2000, Olshausen & Field 2004) by suppressing responses to the most frequently occurring contours. Moreover, theoretical studies have shown that elongated contours in natural images evoke strong statistical dependencies in the responses of V1-like filters, and that near-SM reduces these dependencies (Schwartz & Simoncelli 2001). In support of this hypothesis, we have shown recently that the statistical dependencies in natural images are structured with respect to orientation and spatial frequency in a manner that resembles the orientation and spatial frequency tuning of SM in V1 neurons and human perception (Nurminen & Angelucci 2014). Several other studies have also related SM and neuronal dependencies in V1 (Vinje & Gallant 2000, Vanni & Rosenström 2011, Coen-Cagli et al. 2012). In summary, narrowly tuned near-SM could aid the visual system in forming an efficient representation of natural scenes by increasing the sparseness of the neural responses to natural images and decreasing the statistical dependencies between the responses of V1 neurons. Moreover, as near-surround suppression is strongest when the statistical dependencies between the stimulus in the RF and surround are strongest [i.e., for nearby iso-oriented edges (Nurminen & Angelucci 2014) and for regions belonging to the same object (Coen-Cagli et al. 2012)], a perceptual function that may emerge from near-SM is segmentation of object boundaries.

In contrast, the statistical dependencies in natural images decrease and become only weakly dependent on orientation for distant locations in the image, and far-SM shows a similar distance dependence of its strength and orientation tuning (Nurminen & Angelucci 2014). Moreover, far-SM follows the joint statistics of spatially displaced edges in natural images, being broadly tuned for orientation, just as the more distant parts of natural contours can have a wide distribution of orientations (Geisler et al. 2001). Thus, far-SM suppresses V1 responses to most oriented stimuli at distant image locations, except when the latter are of markedly different orientation (i.e., salient). This property may also serve to enhance salient distant visual targets for guiding saccadic eye movements and attention (Petrov & McKee 2006).

3. CIRCUITS FOR SURROUND MODULATION

Several circuits could generate SM in V1, and current debate is centered on whether this is generated subcortically (in the retina and LGN) or intracortically via intra-V1 horizontal connections, interareal feedback connections to V1, or both. In fact, experimental evidence suggests that feedforward, horizontal, and feedback connections all contribute to SM in V1, but at different spatiotemporal scales (**Figure 2**) and in different cortical layers.

Feedforward connections contribute a temporally fast and untuned component to SM, which spatially is largely restricted to the V1 cell's RF or extends just into the near-surround and emerges first in V1 input layer 4 (4C in monkey). This feedforward component is likely to be the main

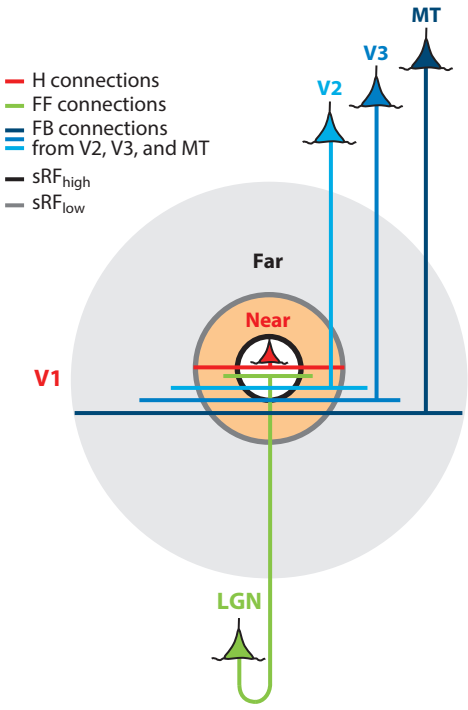

Figure 2

Hypothetical circuits for SM in V1. FF (*green*), H (*red*), and FB (*blue*) connections all contribute to the RF (*white area*) and to near-SM (*orange shaded area*), but only feedback contributes to far-SM (*gray shaded area*), with feedback arising from areas V2, V3, and MT contributing to progressively more distant surround regions. Figure modified from Angelucci et al. (2002). Abbreviations: FB, feedback; FF, feedforward; H, horizontal; SM, surround modulation; sRF$_{high}$ and sRF$_{low}$, summation receptive field measured at high or low contrast, respectively.

substrate generating the small, weaker, and untuned SM of neurons in V1 layer 4 (4C). Horizontal and feedback connections, instead, contribute spatially more extensive tuned components to SM, which are generated outside layer 4C and later in time than untuned SM in 4C. Moreover, although both horizontal and feedback circuits contribute to near-SM, only feedback connections generate far-SM. Below, we review evidence supporting this hypothesis.

3.1. Feedforward Connections

Geniculocortical afferents to V1 are thought to contribute primarily to the spatial and tuning properties of V1 neurons' RFs (Hubel & Wiesel 1962, Reid & Alonso 1995, Angelucci & Sainsbury 2006, Lien & Scanziani 2013), but experimental evidence suggests they also contribute to SM. First, both retinal ganglion cells (Solomon et al. 2006) and LGN cells (Levick et al. 1972, Solomon et al. 2002, Bonin et al. 2005, Sceniak et al. 2006, Alitto & Usrey 2008) exhibit SM. As LGN RFs are smaller than V1 RFs, even a stimulus of optimal size for a V1 cell involves the surround of, and therefore suppresses, LGN cells, resulting in withdrawal of feedforward excitation to V1. Second, pharmacological blockade of inhibition within V1 in cat (through which long-range intracortical connections presumably cause surround suppression) does not abolish near-surround suppression in V1 cells (Ozeki et al. 2004), suggesting that at least some suppression is inherited from LGN.

Collinear facilitation: neuronal response enhancement caused by stimulating the near-surround with lines iso-oriented and collinearly aligned to a line inside the RF

In fact, in cats and primates, SM in LGN and the main geniculate recipient V1 layer (4/4C) share similar properties: Both are spatially restricted, weakly suppressive, and untuned or poorly tuned for orientation (Solomon et al. 2002; Webb et al. 2002; Bonin et al. 2005; Ozeki et al. 2009; Shushruth et al. 2009, 2013), suggesting that near-SM in layer 4/4C may be inherited from SM in LGN. In contrast, SM in V1 supragranular layers is sharply orientation tuned (Hashemi-Nezhad & Lyon 2012, Henry et al. 2013, Shushruth et al. 2013) and therefore cannot be inherited from LGN but must be generated intracortically, likely within the supragranular layers. Moreover, in primates, SM outside V1 layer 4C is spatially more extensive than in LGN and 4C, extending well beyond the visuotopic spread of geniculocortical afferents (Angelucci & Sainsbury 2006) (**Figure 2**), again suggesting a contribution of intracortical circuits to SM outside V1 layer 4C.

In mouse, in contrast to cat and primate, LGN afferents could instead contribute to tuned SM in V1. This is because in mouse, a large fraction of LGN cells have orientation- and direction-selective RFs (Marshel et al. 2012, Piscopo et al. 2013, Scholl et al. 2013, Zhao et al. 2013), and orientation-tuned surround suppression emerges in layer 4 as fast as in other V1 layers and does not require intact superficial layers (Self et al. 2014).

3.2. Horizontal Connections

Horizontal connections in V1 are millimeters-long, intralaminar axonal projections most prominent in lower layers 2/3 and in layer 5 in many mammalian species (Rockland & Lund 1982, 1983; Gilbert & Wiesel 1983). Their features, at least in layers 2/3 (where they have been characterized most extensively), are well suited to generate orientation-tuned near-SM, including both suppressive and facilitatory modulations. First, they arise from excitatory pyramidal cells that extend their axons horizontally beyond the dimensions corresponding to their RF, encompassing a visuotopic extent that is 2–3 times the diameter of their sRF_{high} and commensurate with the size of their near-surround (Angelucci et al. 2002) (**Figure 2**). Second, they target both excitatory and inhibitory neurons (McGuire et al. 1991). Third, at least in layers 2/3, they link preferentially neurons of similar orientation preference (Ts'o et al. 1986, Gilbert & Wiesel 1989, Malach et al. 1993, Ko et al. 2011, Denman & Contreras 2014) along an orientation axis in space that is collinear with the orientation preference of the connected cells (Bosking et al. 1997, Schmidt et al. 1997, Sincich & Blasdel 2001); this property is useful to generate orientation-tuned SM and collinear facilitation (Kapadia et al. 1995, Polat et al. 1998, Chisum et al. 2003, Shushruth et al. 2012). Consistent with the existence of orientation-specific horizontal connections in supragranular layers, near-SM in many species is more sharply tuned for orientation in the supra- than infragranular layers (Hashemi-Nezhad & Lyon 2012, Shushruth et al. 2013), and, in primates, orientation-tuned near-SM emerges earlier in time in supragranular layers (see Section 3.3.1). Notably, computational modeling has revealed that orientation-specific long-range connections are necessary to generate orientation-tuned SM; however, the independence of this tuning from the neurons preferred orientation (as pointed out in Section 2.1) requires the interaction of orientation-tuned surround pathways with local recurrent network (Shushruth et al. 2012; see also Sections 4.1 and 4.3). Weaker tuning of SM in infragranular layers suggests less orientation-specific horizontal connections in these layers; however, we lack information regarding the functional organization of horizontal connections in infragranular layers.

Two recent optogenetic studies in mouse have provided direct evidence for a contribution of intra-V1 horizontal connections to SM in V1 (Adesnik et al. 2012, Sato et al. 2014), indicating that in mouse, orientation-tuned SM is not entirely inherited from the LGN. We argue, however, that these connections contribute to tuned near-SM but not far-SM. In primates, the monosynaptic extent of horizontal connections is insufficient to account for the spatial extent

of the far-surround (Angelucci et al. 2002). Polysynaptic chains of horizontal axons are unlikely to generate far-SM because their conduction velocity, at least in the superficial layers (0.1–0.3 m/s), is too slow (Grinvald et al. 1994, Bringuier et al. 1999, Girard et al. 2001, Slovin et al. 2002, Benucci et al. 2007) to account for the fast onset of far-SM in V1 cells (10–30 ms; see Section 2.1; for a detailed discussion, see Angelucci & Shushruth 2013) and in human perception (Kilpelainen et al. 2007). It remains to be determined whether horizontal axons in infragranular layers have faster conduction velocities (1 m/s) (Girard et al. 2001) that could account for far-SM in these layers. However, because far-SM in infragranular layers is poorly tuned for orientation, it is unlikely that tuned far-SM in supragranular layers can be generated in infragranular layers.

Cytochrome oxidase: a mitochondrial enzyme typically used to identify functional compartments within cortical areas based on its characteristic laminar and columnar distribution

3.3. Feedback Connections

In primates, V1 receives interareal feedback connections primarily from areas V2, V3/VLP, V5/MT, and V6/DM, which arise from layers 2/3A and 5/6 of extrastriate cortex (Kennedy & Bullier 1985, Perkel et al. 1986, Rockland & Virga 1989, Rockland 1994, Rockland & Knutson 2000, Galletti et al. 2001, Angelucci et al. 2002) and terminate primarily in V1 layers 1–2A and 5B–6 (Rockland & Pandya 1979, Federer et al. 2015). The properties of feedback connections are well suited to generate far-SM. First, they arise from excitatory neurons and target both excitatory and inhibitory neurons in V1 (Gonchar & Burkhalter 2003, Anderson & Martin 2009, Zhang et al. 2014), which enables them to both facilitate and suppress V1 cells' responses. Second, they are spatially coextensive with the far-surround of V1 cells, with feedback from areas V2, V3, and MT providing progressively larger feedback terminal fields to V1 (**Figure 2**), corresponding on average to 5, 10, and 25 times, respectively, the sRF_{high} diameter of the targeted V1 cells (Angelucci et al. 2002). Third, feedback axons conduct signals 10 times faster (2–6 m/s) than intra-V1 horizontal axons (Girard et al. 2001), which enables them to mediate the fast onset of far-SM (see Section 2.1).

The functional specificity of feedback connections is controversial. Studies in primates using poorly sensitive anterograde tracers (tritiated amino acids, WGA-HRP, or first-generation adenoviral vectors) or retrograde tracers reported that feedback axons form diffuse terminations in V1 that are not orientation specific (i.e., they contact a diversity of orientation-preference columns) (Rockland & Pandya 1979, Maunsell & Van Essen 1983, Kennedy & Bullier 1985, Perkel et al. 1986, Stettler et al. 2002). In contrast, studies using more sensitive bidirectional tracers (CTB, BDA) have reported clustered and orientation-specific feedback terminations to primate V1 (Angelucci et al. 2002, Shmuel et al. 2005). However, bidirectional tracers label reciprocal pathways, as they are transported both anterogradely and retrogradely; therefore, these studies could not resolve whether the clusters of labeled axon terminals reflected anterogradely labeled feedback terminations, retrogradely labeled axon collaterals of the reciprocal feedforward pathways (known to be clustered), or both.

Recent advances in neuroanatomical labeling, based on viral vectors to deliver genes for fluorescent proteins (Callaway 2008, Nassi et al. 2015), have made it possible to label neurons unambiguously and at high resolution. Ongoing anatomical studies, using viral-based anterograde labeling of V2-to-V1 feedback connections in primates, are revealing clustered and functionally specific feedback connections to V1. In particular, V2-to-V1 feedback appears to be organized into parallel channels related to distinct cytochrome oxidase compartments and to distinct functional maps within each compartment (Federer et al. 2015). Orientation-specific feedback connections are well suited to generate tuned far-SM in supragranular layers. The latter, however, is poorly tuned in the infragranular layers, and further studies are necessary to determine whether feedback to deep layers is less functionally specific than feedback to supragranular layers.

In summary, our hypothesis is that SM is generated by multiple connection types forming a continuum of spatial scales, beginning with feedforward and horizontal connections in V1 providing SM from just outside the RF, and feedback from progressively higher areas providing modulation from progressively more distant surround regions. Therefore, near-SM is generated by all these connection types, but far-SM only by feedback, with feedback from V2 providing the modulation from the most proximal regions of the far-surround, and feedback from MT from the most distal regions of the far-surround (**Figure 2**). Moreover, feedback connections from different areas likely modulate V1 responses in a stimulus-specific fashion, depending on the function of the specific cortical area providing feedback inputs to V1.

Local field potential (LFP): low-frequency voltage signal recorded extracellularly; thought to arise from synaptic activity and subthreshold signals in ensembles of neurons

Current source density (CSD) analysis: second spatial derivative of the LFP signal used to localize the source of the current generating the measured potentials

3.3.1. Distinct laminar processing of near- and far-surround stimuli. In primates, magnocellular and parvocellular geniculocortical afferents terminate predominantly in layer 4C, horizontal connections are most prominent in layers 2/3 and 5, and feedback connections terminate predominantly in layers 1–2A and 5B–6 (**Figure 3**). One can take advantage of this laminar specificity to infer the circuitry for SM. If indeed visual signals in the near- and far-surround are generated by distinct circuits, then stimulation of the near- or far-surround should evoke the earliest postsynaptic depolarization in layers where these circuits terminate.

M. Bijanzadeh, L. Nurminen, S. Merlin & A. Angelucci (submitted manuscript) tested the above prediction. Using linear electrode arrays, they recorded simultaneously through all layers of macaque V1 the local field potential (LFP) evoked by small uniform black square stimuli or static annular gratings flashed at progressively larger distances from the aggregate RF of neurons in the recorded V1 column. Stimuli presented outside the RF of the recorded neurons, in the absence of simultaneous RF stimulation, do not evoke significant spiking responses from the recorded

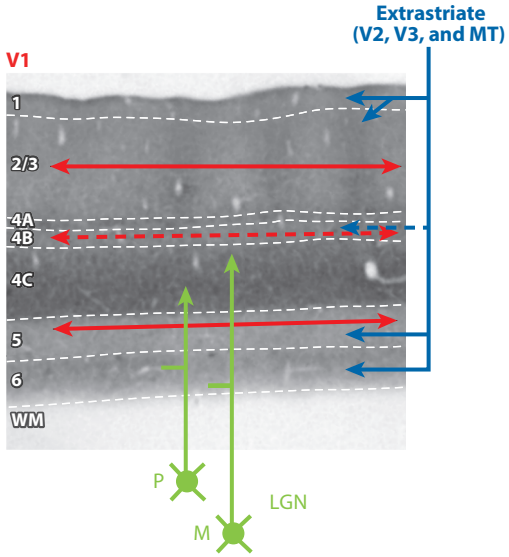

Figure 3

Laminar specificity of feedforward, horizontal, and feedback projections. The main V1 laminar terminations of geniculocortical (*green arrows*), intra-V1 horizontal (*red arrows*), and feedback (*blue arrows*) connections are shown on a pia-to-WM section of V1 stained for cytochrome oxidase. Solid arrows indicate denser projections and dashed arrows weaker projections. White dashed contours indicate laminar boundaries. Abbreviations: LGN, lateral geniculate nucleus; M, magnocellular LGN inputs; P, parvocellular LGN inputs; WM, white matter.

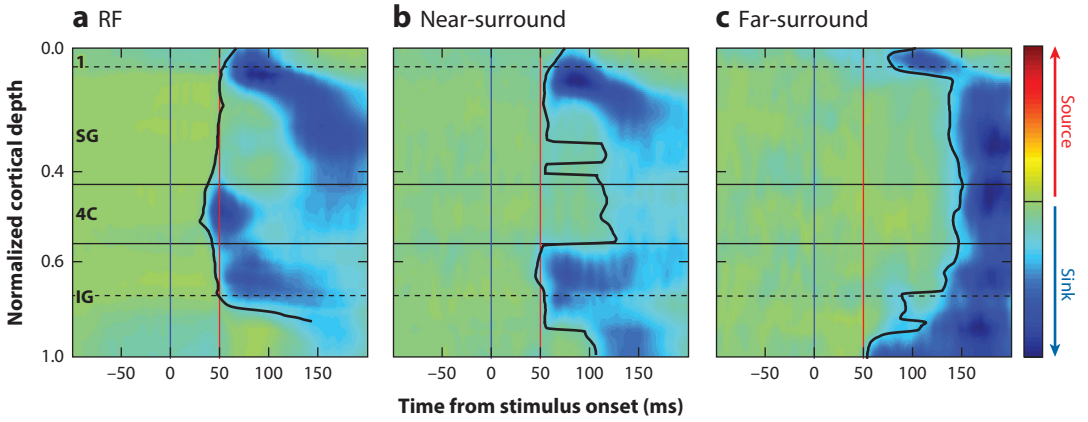

Figure 4

Onset latency of CSD signals evoked by stimulation of the RF, near-surround, or far-surround. Population averages of baseline-corrected (z-scored) CSD signals across V1 layers evoked by stimulation of (*a*) the aggregate RF, (*b*) the near-surround, and (*c*) the far-surround of neurons in the recorded center V1 column. Prior to averaging, CSD signals from each penetration were half-wave rectified to eliminate current sources, and then normalized. The solid black contour indicates the measured onset latency of current sinks, and the blue and red vertical lines mark the time of stimulus onset and 50 ms after stimulus onset, respectively. Horizontal lines mark the main cortical boundaries. Figure modified from M. Bijanzadeh, L. Nurminen, S. Merlin & A. Angelucci (submitted manuscript). Abbreviations: 4C, layer 4C; CSD, current source density; IG, infragranular layers; RF, receptive field; SG, supragranular layers.

neurons; therefore, the LFPs recorded in the center nonstimulated column reflect presynaptic input activity and postsynaptic subthreshold responses evoked by surround-only stimuli. To localize these subthreshold responses to specific layers, these authors applied current source density (CSD) analysis to the LFP signals and measured the onset latency of current sinks across layers. Current sinks are negative voltage deflections in CSD representing the net depolarization of neurons at a particular local site (Mitzdorf 1985). These authors found that when a small square stimulus was flashed inside the RF, the earliest current sinks occurred in layer 4C, where geniculocortical inputs predominantly terminate (**Figure 4*a***). As the stimulus was progressively moved away from the RF, CSD signals in layer 4C were delayed, and stimuli closer to the RF evoked the earliest current sinks almost simultaneously in supra- and infragranular layers (**Figure 4*b***), whereas more distant surround stimuli evoked the earliest current sinks in layers 1 and 6 (**Figure 4*c***). Because layers 1 and 6 are the primary targets of feedback connections (**Figure 3**), these results suggest that visual signals in the far-surround are relayed to the center column via feedback connections, and therefore that far-SM is initiated by feedback. In contrast, stimuli in the near-surround are relayed to the center column by a variety of connection types, possibly including both horizontal, interlaminar, and feedback connections, as these stimuli evoked subthreshold input activity almost simultaneously in all layers, except geniculate recipient layer 4C.

Bijanzadeh et al. also measured the onset latency of untuned and orientation-tuned near- and far-surround suppression of spiking responses evoked by the same surround stimuli described above, but presented together with a grating stimulus inside the aggregate RF of neurons in the recorded V1 column. They found that untuned near-surround suppression first emerged in layer 4C, again suggesting a geniculocortical contribution. Tuned near-surround suppression first emerged in supragranular layers, suggesting it is generated by orientation-specific horizontal (and possibly feedback) connections within these layers. Far-surround suppression emerged first and almost simultaneously in supra- and infragranular layers, and latest in layer 4C, a layer that lacks horizontal and feedback connections and whose neurons largely confine their dendrites

within this layer. Because far-surround stimuli evoke the earliest subthreshold activity in feedback recipient layers 1/2A and 6 (**Figure 4*c***), far-surround suppression of spiking responses in supra- and infragranular layers must be initiated by feedback contacts with inhibitory cells in these layers. In turn, inhibitory neurons in superficial layers can suppress pyramidal cells in most layers (except 4C and 6), via contacts with these cells' apical dendrites ascending to layer 1. Layer 4C instead could inherit late far-surround suppression from other layers via interlaminar connections.

3.3.2. The role of feedback connections: inactivation studies. Several studies have investigated the impact on SM in V1 of inactivating feedback connections by pharmacologically silencing or cooling extrastriate cortex. These studies have produced contrasting results. On the one hand, some studies have observed weak reduction in surround suppression after cooling primate MT (Hupé et al. 1998) or V2 and V3 together (Nassi et al. 2013), or cat posterotemporal visual cortex (the presumed homolog of primate inferotemporal cortex) (Bardy et al. 2009). On the other hand, other studies have observed general reduction in response gain with no changes in SM after pharmacologically silencing primate V2 (Hupé et al. 2001), cooling cat posterotemporal visual cortex (Wang et al. 2010), or optogenetically silencing mouse cingulate cortex (Zhang et al. 2014).

These inactivation approaches, however, did not perturb feedback neuron activity selectively, but rather affected activity in an entire cortical area and therefore could not rule out that the observed effects resulted from indirect pathways through the thalamus or other cortical areas. Moreover, these approaches lacked temporal precision (acting on a time scale of minutes to hours, whereas neurons act on a time scale of milliseconds) and did not allow fine control of inactivation levels, thus precluding potentially more physiologically relevant manipulations and leaving open the possibility that the discrepant results reflected different levels of inactivation.

Recently, Nurminen et al. (2016) reinvestigated the role of V2-to-V1 feedback connections in SM using optogenetics, which, in contrast to previous inactivation methods, allows for selective inactivation of feedback neuron and for fine control of inactivation levels at millisecond time resolution (Zhang et al. 2007). These authors inactivated V2 feedback terminals in the superficial (but not deep) V1 layers by directing green laser light of increasing intensities to V1 while recording at the photoactivated V1 site neuronal responses to grating stimuli of increasing size (**Figure 5*a*,*b***). Notably, inactivation of feedback from V2 was expected to mostly affect SM arising from the near-surround and the more proximal region of the far-surround, but not the most distal parts of the far-surround, because feedback from V3 and MT (which is spatially more extensive than feedback from V2; **Figure 2**) was unperturbed. These authors found that at low light intensities, V2 feedback inactivation caused a shift of the size-tuning peak toward larger stimuli (i.e., an increase in RF size), which, in about 50% of the cells, was accompanied by an increase in the height of the peak (**Figure 5*c***). Owing to this shift, the response to stimuli inside the RF was reduced, and surround suppression was reduced in the more proximal (but not most distal) surround regions (**Figure 5*c***).

Higher laser intensities, instead, caused general response reduction to all stimulus sizes (**Figure 5*d***), particularly in the supragranular layers, where effective laser irradiance is higher than in deeper layers. This result suggests that the discrepant and variable effects observed across previous studies can be attributed to different levels of feedback inactivation achieved in different studies.

Beyond supporting a role for feedback in SM, the study by Nurminen et al. (2016) has identified the cellular-level basis of how feedback affects information processing in V1 (i.e., by modulating RF size, surround suppression, and response gain). Notably, several forms of top-down influences in visual processing, such as spatial attention, have been shown to affect neuronal responses in a similar fashion (McAdams & Reid 2005, Ito & Gilbert 1999, Roberts et al. 2007), suggesting that these effects are mediated by top-down modulations of feedback to V1.

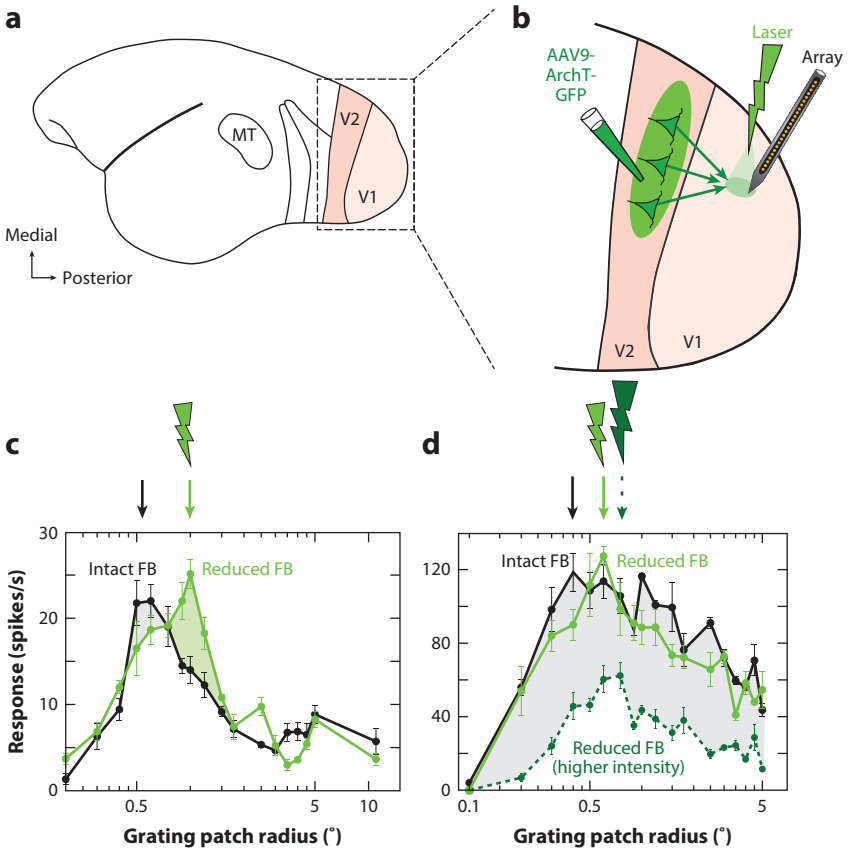

Figure 5

Optogenetic inactivation of V2 feedback affects receptive field size, surround suppression, and response gain in V1 neurons. (*a*) Lateral view of the marmoset brain. Areas V1 and V2 inside the boxed region are shown enlarged in panel *b*. (*b*) The inactivation paradigm. Area V2 was injected with AAV9 expressing the genes for the inhibitory opsin ArchT and GFP. Laser photoactivation of ArchT-expressing V2 feedback terminals was directed to V1 while V1 neuron responses were recorded using linear electrode arrays at the photoactivated site. (*c*) Size-tuning curve of an example V1 cell recorded with intact (*black*) and reduced (*green*) V2 feedback activity. The gray shaded area highlights the response reduction to stimuli inside the RF. The green shaded area highlights the response increase (reduced suppression) in the proximal surround region. (*d*) Size-tuning curve of an example V1 cell measured with intact feedback (*black*) and with reduced feedback activity (*green*) using laser stimulation at two different intensities (*dashed curve*: higher laser intensity). Other conventions as in panel *c*. Figure modified from Nurminen et al. (2016). Abbreviations: AAV9, adeno-associated virus; FB, feedback; GFP, green fluorescent protein.

4. MECHANISMS FOR SURROUND MODULATION

Here we present a working hypothesis on the mechanisms for SM inspired primarily by theoretical modeling and evaluate this hypothesis against recent experimental evidence.

The studies reviewed above support the idea that SM in V1 results from multiple mechanisms. It consists of a fast and spatially restricted untuned component, which emerges in layer 4C and is inherited from LGN owing to surround suppression of LGN cells. It also consists of a slower and more extensive tuned component, which emerges outside layer 4C and results from interactions of horizontal and feedback connections with local circuits. Although the specific mechanisms

underlying these interactions remain to be elucidated, theoretical studies and experimental data have led us to the computational model described below. Modifications and refinements to this model are expected as more data on inhibitory neurons' function and connectivity and the synaptic mechanisms for SM become available. For now, we view this model as a work-in-progress, theoretical framework to guide experimental design and interpretation of results.

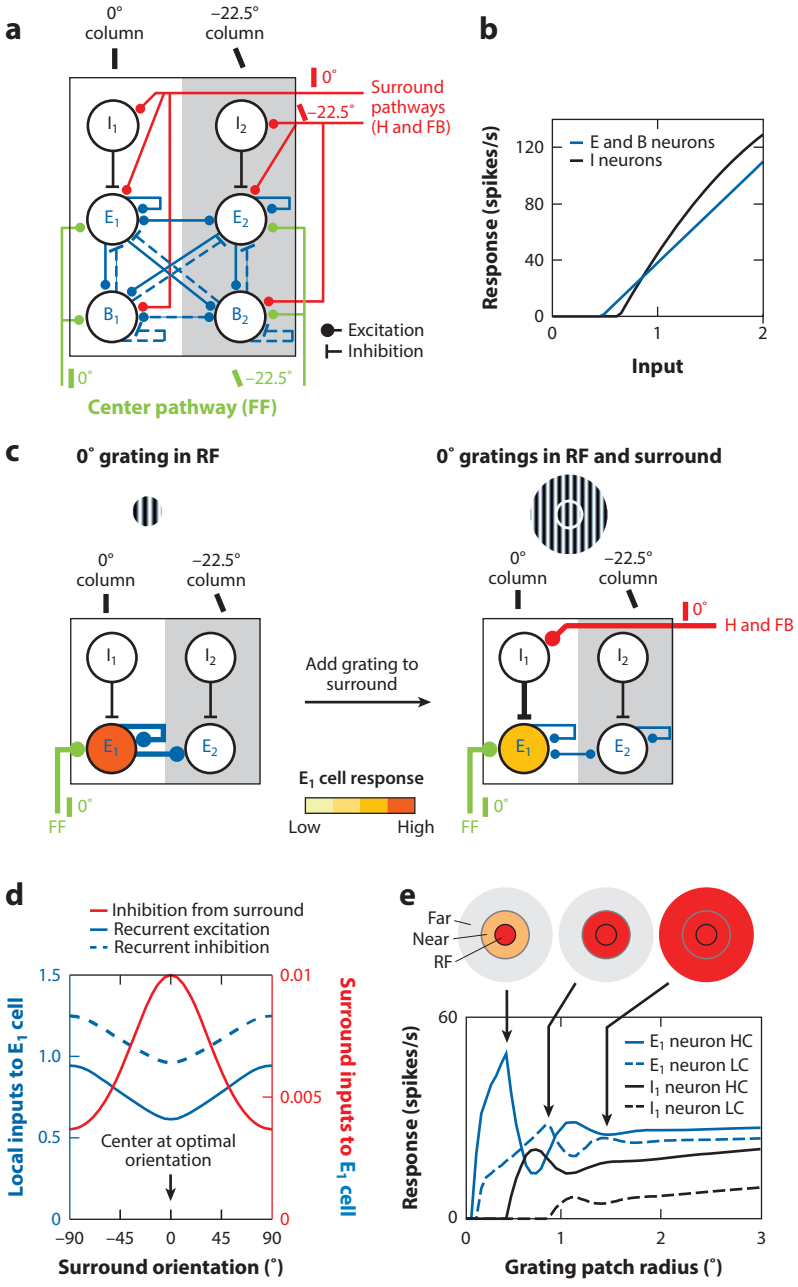

4.1. A V1 Model of Surround Modulation: A Working Hypothesis

We first describe the model architecture and then explain how SM is generated in the model.

Hypercolumn: An orientation hypercolumn in V1 is a region of cortex encompassing a full set of orientation-preference columns

4.1.1. Model architecture. We describe a model of orientation-tuned SM in layer 2/3 of macaque V1 (Schwabe et al. 2006, Shushruth et al. 2012). In the model, stimuli in the RF surround activate horizontal and feedback connections, which, in turn, modulate the local recurrent network within the center V1 hypercolumn via orientation-specific excitatory contacts with both excitatory (E) and inhibitory neurons (**Figure 6*a***). The current model includes two types of inhibitory neurons (following Bressloff & Cowan 2002): local (I) and basket-like neurons (B). The I neurons receive surround inputs (both horizontal and feedback) from outside the orientation hypercolumn and contact only E neurons within the same orientation column; therefore, they are tuned for orientation. The I neurons' main role is to relay the suppressive influences from the surround to the center column (lateral inhibition). B neurons receive orientation-specific feedforward, horizontal, and feedback inputs and make recurrent connections with themselves and other E and B cells between different orientation columns within the same hypercolumn; therefore, they are poorly orientation-tuned. Their role is to sharpen orientation-tuning within the column and to balance the strong recurrent excitation (recurrent feedback inhibition). E neurons in the model also make broadly tuned local recurrent connections with themselves and other E and B neurons. Importantly, the model is operated in a regime of strong recurrency with balanced recurrent excitation and inhibition, an assumption based on theoretical and experimental studies suggesting the cortex operates in such a regime (see Section 4.2). A second important assumption is that the response of the I neurons is asymmetric relative to the response of the E and B neurons. This asymmetry is such that for weak visual inputs, I neurons are silent, so that excitatory inputs from the surround to the center column increase the E/B neurons' response, whereas for strong visual inputs, I neurons

Figure 6

A recurrent network model of SM in layer 2/3 of macaque V1. (*a*) The network architecture. A center hypercolumn consisting of 32 recurrently connected orientation columns, of which only 2 (preferring 0° and −22.5° orientation) are shown for simplicity. Each column consists of excitatory neurons (E) and two kinds of inhibitory neurons (I and B). The surround pathways (*red*) are orientation specific, whereas the local recurrent connections (*blue*) are broadly tuned. Feedforward projections (*green*) from layer 4C are also orientation specific and contact E and B, but not I, neurons. (*b*) Input/response function of E, B, and I neurons in the model. (*c*) The mechanism underlying orientation-tuned surround suppression. Diagrams show the inputs that most affect the E_1 cell response for a center stimulus at the optimal orientation (0°) for cell E_1 (*left*) and after addition of a surround stimulus at 0° orientation (*right*). Only the relevant cells and connections that most affect the E_1 cell response in the model are depicted. Line thickness indicates input strength. Adding a 0° grating to the surround leads to increased inhibition of the E_1 cell via the surround inputs, which in turn leads to less recurrent excitation within the hypercolumn, as E_1 provides the strongest recurrent excitation within the hypercolumn when a center stimulus of 0° (its preferred orientation) is presented. (*d*) Inputs to the E_1 cell preferring 0° orientation for varying surround orientations, when the RF is stimulated with a center grating at the optimal orientation for the recorded cell. Local recurrent inputs from E neurons in other orientation columns (*solid blue curve*), local recurrent inputs (negative) from B neurons in the same and other orientation columns (*dashed blue curve*), and input (negative) from the surround (*red curve*) are shown. Note that the surround input (*red* y-*axis*) is much smaller than the local recurrent inputs (*blue* y-*axis*). (*e*) Contrast-dependent spatial summation in the model. Size-tuning curves at high (85%) and low (15%) contrast are shown. Icons at top indicate different components of the RF and surround activated (*red shading*) at the indicated point in the size-tuning curve. Panels *a*–*d* modified from Shushruth et al. (2012); panel *e* modified from Schwabe et al. (2006). Abbreviations: B, basket-like inhibitory cell; E, excitatory cell; FB, feedback; FF, feedforward; H, horizontal; HC, high contrast; I, local inhibitory cell; LC, low contrast; RF, receptive field; SM, surround modulation.

are active, and excitatory inputs from the surround suppress the E and B neurons' response. This asymmetry in our model (Schwabe et al. 2006, Shushruth et al. 2012), as in previous models (Lund et al. 1995, Somers et al. 1998), is implemented as I neurons having higher threshold and gain than E and B neurons (**Figure 6*b***), but other implementations are conceivable (see Section 4.2).

4.1.2. Circuit and synaptic mechanisms generating orientation-tuned surround modulation in the model. Surround stimulation causes an increase in horizontal activity, feedback activity, or both, which in turn leads to an increase in the activity of I, E, and B neurons in the center column matching the orientation of the surround stimulus. As I neurons are more strongly activated by horizontal and feedback connections than B and E neurons, initial suppression of the E neurons dominates and, in turn, owing to the strong recurrent connections between E and B cells, leads to a reduction in recurrent excitation and inhibition within the whole hypercolumn (because the E and B cells provide recurrent connections to the entire hypercolumn). Suppression occurs despite reduced B inhibition, which counteracts the decreased excitation, because of the overall net reduction in excitation (**Figure 6*c*,*d***). In summary, surround suppression in this model results from an active increase in I inhibition, causing a decrease in recurrent excitation and B inhibition that dominates over the increased I inhibition at steady state, owing to the strong recurrent regime (**Figure 6*d***).

The strong recurrent regime in the model is crucial to account for the experimental observation that surround suppression is strongest when the center and surround are stimulated at the same orientation, irrespective of the preferred orientation of the recorded cell (Shushruth et al. 2012). This is because maximal withdrawal of recurrent excitation within the center hypercolumn occurs when the surround pathways (which are orientation specific) inhibit the E neurons in the center orientation column that provide the strongest recurrent excitation to the whole hypercolumn; this occurs at any stimulus orientation, as long as the center and surround stimuli are iso-oriented.

The I neuron response asymmetry (**Figure 6*b***) in the model is what accounts for the contrast dependence of SM [i.e., facilitation at low contrast and suppression at high contrast (see Section 2.1)] as well as the expansion of the sRF size at low contrast (**Figure 1**). At low contrast, the I neurons are silent and E and B neurons can integrate excitatory signals over larger stimuli before the threshold for I inhibition is reached and suppression occurs (**Figure 6*e***). The same mechanism can also account for the expansion of the sRF size when excitatory feedback inputs to V1 are reduced by optogenetic inactivation of feedback (**Figure 5*c***; see Section 3.3.2; Nurminen et al. 2016).

4.2. Biological Plausibility of the Model

Here we evaluate the role of inhibition and the connectivity in the model against available experimental data.

4.2.1. Inhibitory neurons. The model I and B neurons share many of the properties described for the somatostatin (SOM) and parvalbumin (PV) neurons, respectively, of the mouse sensory cortex. SOM neurons exhibit stronger orientation selectivity (as in the model), weaker spontaneous and evoked firing activity, and longer response latencies than PV neurons (Ma et al. 2010). Their delayed response to feedforward excitation, and their preferential synaptic contacts onto distal dendrites of pyramidal cells (Silberberg & Markram 2007, Ascoli et al. 2008), where horizontal and feedback excitatory inputs are more likely localized (Kisvárday et al. 1986, McGuire et al. 1991, Anderson & Martin 2009, Petreanu et al. 2009), suggest SOM cells interact with later arriving intracortical (modulatory) excitatory inputs. Recent optogenetic studies have directly demonstrated a causal role for SOM neurons in horizontal- and feedback-mediated surround

suppression in mouse V1 (Adesnik et al. 2012, Nienborg et al. 2013, Zhang et al. 2014). Whereas SOM neurons in both supra- and infragranular layers contact both pyramidal and other types of inhibitory neurons (Pfeffer et al. 2013, Jiang et al. 2015), in layers 2/3 their connection probability with pyramidal cells is twice that with PV cells, and, functionally, the dominant effect of SOM neuron activation in layers 2/3 is inhibition of pyramidal neurons (Xu et al. 2013). In our model, this is simplified by having I neurons connect exclusively with E neurons (**Figure 6*a***), but it is clear that future modifications of the model will have to include SOM-to-PV connections.

In mouse visual cortex, PV neurons, as in the model, are poorly orientation tuned (Ma et al. 2010); form recurrent connections with other PV and E, but not other inhibitory, neurons (feedback recurrent inhibition) (Pfeffer et al. 2013, Jiang et al. 2015); and are involved in balancing recurrent excitation as well as mediating feedforward inhibition and gain control (reviewed in Tremblay et al. 2016). In our model, PV neurons also serve to sharpen orientation-tuned responses; however, there has been disagreement as to whether SOM (Wilson et al. 2012) or PV (Lee et al. 2012) neurons play this role. More recently, research has shown that the specific suppressive function of both inhibitory neuron types can be flexible and dependent on the response mode of the neurons, the property of the network within which they are embedded, and the nature of visual stimuli and stimulation protocols (El-Boustani & Sur 2014, Lee et al. 2014, Seybold et al. 2015, Phillips & Hasenstaub 2016).

I model neurons have higher threshold and response gain than E and B neurons and thus show weaker responses than E and B neurons to weak (e.g., small or low-contrast) visual stimuli (**Figure 6*b***), and this accounts for the nonlinear changes in SM. On the one hand, in contrast to our model, SOM neurons in layer 5 have low spiking threshold, but a variety of other physiological response properties have been described for SOM cells in other layers (Kawaguchi & Kubota 1997, Ma et al. 2006, Xu et al. 2013). On the other hand, SOM neurons show other features, such as facilitating synapses and large RF size, that may provide them with the response asymmetry needed in the model to account for the nonlinear changes in SM. Specifically, in contrast to PV neurons, SOM neurons have slow membrane time constant and facilitating excitatory inputs (Reyes et al. 1998, Kapfer et al. 2007, Silberberg & Markram 2007), which lead to delayed responses and increase in spike probability upon repetitive stimulation. These properties cause slower recruitment of SOM neurons, compared to PV and pyramidal neurons, and allow them to summate excitatory postsynaptic potentials (EPSPs) and produce supralinear responses (similar to the model I neurons; **Figure 6*b***). Moreover, SOM neurons have much larger RFs than PV and pyramidal neurons; thus, similar to the model I neurons (**Figure 6*e***), small stimuli evoke weaker responses in SOM neurons, compared to PV and pyramidal neurons, whereas large stimuli evoke maximal responses in SOM neurons, in turn leading to suppression of PV and pyramidal neurons (Adesnik et al. 2012).

4.2.2. Alternative mechanism for asymmetric inhibition. Our model accounts for the nonlinear changes in SM using high-threshold/gain I/SOM interneurons. In the model of Rubin et al. (2015), instead, the nonlinear changes in SM are implemented using a fundamentally different mechanism based on a supralinear input/output (I/O) function of cortical neurons (Priebe & Ferster 2008), which causes the gain of the I/O function to increase with increasing postsynaptic activity. For weak stimuli, the neurons are weakly coupled, and their inputs are dominated by external drive, so multiple stimuli add supralinearly. For strong stimuli, network drive dominates, the strong recurrent excitation becomes unstable, but recurrent feedback inhibition stabilizes it (inhibition-stabilized network or ISN), largely canceling out the external input and leading to sublinear summation of multiple presented stimuli (i.e., surround suppression). Thus, with increasing input drive, the network becomes more dominated by inhibition. One current

limitation of the Rubin et al. (2015) model is that it considers only one class of interneuron (similar to the B cells of our model) and thus cannot account for some of the features of our model, which arise from having two inhibitory neuron types with distinct properties and functions (see Section 4.3 below). However, it should be straightforward to incorporate SOM neurons into an ISN model (Ken Miller, personal communication). Although the precise mechanism for the nonlinear changes in SM remains hypothetical, this does not affect the major underlying assumptions of our model, namely that the various forms of surround suppression are a consequence of cortical networks operating in a strongly recurrent and balanced regime, with more than one type of interneuron and a combination of feedforward, horizontal, and feedback connections.

4.2.3. Connectivity. In our model, the spatial scale, conduction velocities, and orientation specificity of horizontal and feedback connections are based on the experimental data reviewed in Section 3. As in the model, in real life, feedforward connections from the granular layer to layer 2/3 contact PV and excitatory cells (feedforward inhibition) but not SOM neurons (Dantzker & Callaway 2000, Gonchar & Burkhalter 2003, Adesnik et al. 2012). In the model, feedback connections contact excitatory as well as all interneuron types, and surround suppression is initiated by increased SOM neuron activity; this is consistent with data in mouse, showing that feedback connections to V1 from cingulate cortex target excitatory and all three major types of inhibitory neurons [PV, SOM, and vasoactive-intestinal peptide (VIP)], and that feedback-mediated surround suppression occurs primarily via contacts with SOM neurons (Zhang et al. 2014). Horizontal connections have been shown to contact both excitatory and SOM neurons but to activate SOM neurons more strongly (Adesnik et al. 2012). However, more exhaustive studies are needed to determine whether other inhibitory neuron types are also targeted by horizontal connections in V1; thus, in our model, we assume that feedback and horizontal connections target the same cell types.

Future model extensions will need to include additional inhibitory neuron types, in particular VIP neurons, a major target of feedback connections (Gonchar & Burkhalter 2003, Zhang et al. 2014). Moreover, it is unclear to what extent the SOM neurons participate in the recurrent networks, as they do not receive much inhibition from other SOM and PV neurons, but they do contact PV and E neurons; thus, future model extension will need to explore how the different properties of these two neuron types (PV and SOM) affect recurrent interactions and cortical dynamics differently. Finally, the model will need to include multiple cortical layers and account for the laminar differences in SM using laminar-specific circuitry.

4.3. Model Predictions

Our model is operated in a regime of strong recurrency with balanced excitation and inhibition. This is because cortical neurons are embedded within recurrent networks, and theoretical and experimental evidence indicates that strong recurrent feedback inhibition shapes the operating regime of the cortex (Wolf et al. 2014). Theoretically, recurrent feedback inhibition is indispensable for stabilizing recurrent excitation, which serves to amplify specific input patterns and generate persistent activity (van Vreeswijk & Sompolinsky 1996, Bressloff et al. 2001, Bressloff & Cowan 2002). Experimental evidence suggests that local inhibitory connections are strong and dense (Fino & Yuste 2011, Hofer et al. 2011, Isaacson & Scanziani 2011) and that some fundamental cortical responses can be explained only if the cortex operates in a regime of strong and balanced recurrent connections (Marino et al. 2005, Ozeki et al. 2009, Stimberg et al. 2009, Shushruth et al. 2012, Chariker et al. 2016).

Strong and balanced recurrent networks, such as our model or the ISN model of Rubin et al. (2015), make the important prediction that above a threshold strength of recurrent excitation and

inhibition, an increased drive to the inhibitory cells leads to a decrease in the firing rates of both excitatory and inhibitory cells at steady state (Section 4.1). Therefore, both recurrent excitation and inhibition received by E cells are expected to decrease when the cells are surround suppressed (**Figure 6*d***). In our model, this reduction in excitation and inhibition is caused by sustained increased activity of I/SOM neurons, which leads to initial increased inhibition of the E neurons and subsequent reduced recurrent excitation and B inhibition. Increased SOM activity can be transient if SOM neurons are part of the recurrent network (as in the model of Rubin et al. 2015) but can be sustained (as shown by Adesnik et al. 2012) if they are not (as in our model); regardless, owing to the strong recurrent regime, in our model reduction of recurrent excitation and inhibition at steady state dominates over the sustained I/SOM increased inhibition (**Figure 6*d***).

The model predicts that blind intracellular recordings (i.e., not targeted to specific neuron types or domains in the cortical orientation map) should reveal net reduction in excitation and inhibition at steady state in most recorded cells (i.e., the E and B, but not I, neurons), but additional transient increases in IPSPs, EPSPs, or both would be observed only in a small fraction of recorded cells. This is because the surround pathways contact the center E_1, I_1, and B_1 neurons in an orientation-specific manner (i.e., the neurons in the center column prefer the same orientation as the stimulus-activated surround pathways; see **Figure 6*a***); therefore activation of the surround leads to transient increases in EPSPs in E_1 and B_1 (but not E_2 and B_2) neurons, sustained increases in EPSPs only in I_1 neurons, and transient increases in inhibitory postsynaptic potentials (IPSPs) only in E_1 neurons.

Intracellular recordings in anesthetized cat and mouse have reported a variety of different effects consistent with these model's predictions. Ozeki et al. (2009) measured EPSPs and IPSPs in cat V1 cells in response to drifting center-surround gratings. In most of the recorded neurons, they found reduced excitation and inhibition at steady state, which could not be explained by suppression of LGN inputs; moreover, the decrease in EPSPs and IPSPs was temporally preceded by a transient increase (lasting 30–50 ms) in inhibition in a small subset of cells whose preferred orientation matched that of the presented stimulus (as the E_1 cells in our model), and few cells showed transient increases in both EPSPs and IPSPs. Sato et al. (2016) combined optogenetic activation of the horizontal network with intracellular recordings from mouse V1 cells presented with gratings inside their RF. They found only reduced excitation and inhibition, which in few cells was preceded by a transient increase in EPSP; they failed to find transient increases in inhibition, possibly because they recorded from only 10 cells. In contrast, Haider et al. (2010) recorded intracellularly from identified regular-spiking pyramidal cells and fast-spiking (presumed inhibitory) neurons in cat V1 while presenting naturalistic movies to the cells' RFs and surround. By averaging IPSP and EPSP amplitude over the stimulus presentation time, in pyramidal cells they found increased average IPSP amplitude, but unchanged average EPSP amplitude, relative to RF-only stimulation. However, their recording traces reveal fluctuations in both EPSPs and IPSPs over stimulus presentation time, with large IPSP increases typically corresponding to large EPSP decreases (e.g., see figure 2 in Haider et al. 2010). In contrast, inhibitory neurons had larger RFs and increased their spiking rate in response to surround stimulation (behaving like the SOM neurons in Adesnik et al. 2012), possibly causing increased IPSP amplitude in pyramidal cells.

Although the studies of Ozeki et al. (2009) and Haider et al. (2010) both emphasize that surround suppression depends on local intracortical inhibition, they disagree as to whether the increased inhibition is transient or sustained. The different results of these studies may be due to the different stimuli used. Grating stimuli, as used in Ozeki et al. (2009) and Sato et al. (2016), are spatiotemporally narrow band and therefore activate only restricted populations of orientation-specific neurons, making it more difficult to record blindly from the E_1 neurons (the cells in which surround stimulation is predicted to evoke increased IPSPs), and causing a more consistent

type of modulation (suppression). In contrast, natural movies, as used in Haider et al. (2010), are broad band, activating much larger populations of neurons in multiple orientation columns, therefore increasing the probability of recording from E_1 neurons (and observing increased IPSPs). However, it remains unclear why Haider et al. (2010) failed to observe a reduction in EPSPs and IPSPs, as seen at steady state in the other two studies and as predicted by recurrent models. One possibility is that the natural movie stimulus keeps the cortex in a continuously changing, transient state, in which cells are facilitated continuously by some frames, suppressed by others, and unchanged by yet others (Sachdev et al. 2012).

5. CONCLUSIONS AND REMAINING QUESTIONS

We have presented theoretical and experimental evidence supporting the notion that SM in the cortex is generated by a complex network of feedforward, horizontal, and feedback circuits interacting with strong and balanced local recurrent connections. Further testing of this hypothesis requires selective optogenetic manipulation of specific circuit types, particularly in higher species, and recording postsynaptic responses in identified neuron types and at specific map locations.

Many questions remain unanswered. One question needing further exploration regards the distinct functional roles of feedback connections arising from different areas and how these differently affect SM. Moreover, we need a better understanding of the circuits and mechanisms underlying the laminar-specific properties of SM. Answering these questions requires knowledge of how the synaptic and functional organization of horizontal and feedback circuits, and the cell types targeted by these circuits, vary across V1 layers. Furthermore, we need to understand the connectivity and functional role of different inhibitory neuron types in higher mammals, as it is not clear to what extent the insights gained from mouse studies translate to cat and primate (see, e.g., Wilson et al. 2017). Recent advances in the application to higher species of viral technology (Dimidschstein et al. 2016) and optogenetics (e.g., Cavanaugh et al. 2012, Gerits et al. 2012, Nurminen et al. 2016) and the possibility of generating transgenic marmosets (Okano et al. 2012) will open new avenues for addressing these challenges. As a general recommendation for future studies, an effort needs to be made to use recurrent network models, such as the one we have proposed here, to guide experiments and interpret their results. Cortical neurons are embedded within dynamical, nonlinear recurrent networks. In contrast to linear feedforward networks, such networks can exhibit a wide variety of complex behavior including multiscale oscillations, multistability, chaotic dynamics (sensitivity to initial conditions), and long-lasting transients. The dynamics can also exhibit dramatic changes in response to small variations in physiological parameters (bifurcations) or optogenetic manipulation. Such complex phenomena often yield counterintuitive results that only modeling can help explain.

DISCLOSURE STATEMENT

The authors are not aware of any affiliations, memberships, funding, or financial holdings that might be perceived as affecting the objectivity of this review.

ACKNOWLEDGMENTS

We thank Drs. Hillel Adesnik, Kenneth Miller, and Robert Shapley for useful discussions and comments on the manuscript. This work was supported by the National Institutes of Health (National Eye Institute grants R01 EY019743 and R01 EY026812 and National Institute of Neurological Disorders and Stroke BRAIN grant U01 NS099702 to A.A.), the National Science Foundation

(grants IOS 1355075 and EAGER 1649923 to A.A. and grant DMS-1613048 to P.C.B.), the University of Utah Research Foundation (seed grant 10040877 to A.A.), the University of Utah Neuroscience Initiative (seed grant to A.A.), a grant from Research to Prevent Blindness to the Department of Ophthalmology, University of Utah, and a postdoctoral fellowship from the Ella and Georg Ehrnrooth Foundation to L.N.

LITERATURE CITED

Adesnik H, Bruns W, Taniguchi H, Huang ZJ, Scanziani M. 2012. A neural circuit for spatial summation in visual cortex. *Nature* 490:226–31

Alitto HJ, Usrey WM. 2008. Origin and dynamics of extraclassical suppression in the lateral geniculate nucleus of the macaque monkey. *Neuron* 57:135–46

Allman J, Miezin F, McGuinness E. 1985. Stimulus specific responses from beyond the classical receptive field: neurophysiological mechanisms for local–global comparisons in visual neurons. *Annu. Rev. Neurosci.* 8:407–30

Anderson JC, Martin KAC. 2009. The synaptic connections between cortical areas V1 and V2 in macaque monkey. *J. Neurosci.* 29:11283–93

Angelucci A, Bressloff PC. 2006. The contribution of feedforward, lateral and feedback connections to the classical receptive field center and extra-classical receptive field surround of primate V1 neurons. *Prog. Brain Res.* 154:93–121

Angelucci A, Levitt JB, Walton E, Hupé JM, Bullier J, Lund JS. 2002. Circuits for local and global signal integration in primary visual cortex. *J. Neurosci.* 22:8633–46

Angelucci A, Sainsbury K. 2006. Contribution of feedforward thalamic afferents and corticogeniculate feedback to the spatial summation area of macaque V1 and LGN. *J. Comp. Neurol.* 498:330–51

Angelucci A, Shushruth S. 2013. Beyond the classical receptive field: surround modulation in primary visual cortex. In *The New Visual Neurosciences*, ed. LM Chalupa, JS Werner, pp. 425–44. Cambridge, MA: MIT Press

Ascoli GA, Alonso-Nanclares L, Anderson SA, Barrionuevo G, et al. 2008. Petilla terminology: nomenclature of features of GABAergic interneurons of the cerebral cortex. *Nat. Rev. Neurosci.* 9:557–68

Bair W, Cavanaugh JR, Movshon JA. 2003. Time course and time–distance relationships for surround suppression in macaque V1 neurons. *J. Neurosci.* 23:7690–701

Bardy C, Huang JY, Wang C, Fitzgibbon T, Dreher B. 2009. "Top-down" influences of ispilateral or contralateral postero-temporal visual cortices on the extra-classical receptive fields of neurons in cat's striate cortex. *Neuroscience* 158:951–68

Barlow HB. 1961. Possible principles underlying the transformation of sensory messages. In *Sensory Communication*, ed. WA Rosenblith, pp. 217–34. Cambridge, MA: MIT Press

Barlow HB. 1972. Single units and sensation: a neuron doctrine for perceptual psychology? *Perception* 1:371–94

Benucci A, Frazor RA, Carandini M. 2007. Standing waves and traveling waves distinguish two circuits in visual cortex. *Neuron* 55:103–17

Berman RA, Wurtz RH. 2011. Signals conveyed in the pulvinar pathway from superior colliculus to cortical area MT. *J. Neurosci.* 31:373–84

Blakemore C, Tobin EA. 1972. Lateral inhibition between orientation detectors in the cat's visual cortex. *Exp. Brain Res.* 15:439–40

Bonin V, Mante V, Carandini M. 2005. The suppressive field of neurons in lateral geniculate nucleus. *J. Neurosci.* 25:10844–56

Born RT, Bradley DC. 2005. Structure and function of visual area MT. *Annu. Rev. Neurosci.* 28:157–89

Bosking WH, Zhang Y, Schofield B, Fitzpatrick D. 1997. Orientation selectivity and the arrangement of horizontal connections in tree shrew striate cortex. *J. Neurosci.* 17:2112–27

Bressloff PC, Cowan JD. 2002. An amplitude equation approach to contextual effects in visual cortex. *Neural Comput.* 14:493–525

Bressloff PC, Cowan JD, Golubitsky M, Thomas PJ, Wiener MC. 2001. Geometric visual hallucinations, euclidean symmetry and the functional architecture of striate cortex. *Philos. Trans. R. Soc. B* 356:299–330

Bringuier V, Chavane F, Glaeser L, Frégnac Y. 1999. Horizontal propagation of visual activity in the synaptic integration field of area 17 neurons. *Science* 283:695–99

Callaway EM. 2008. Transneuronal circuit tracing with neurotropic viruses. *Curr. Opin. Neurobiol.* 18:617–23

Cavanaugh JR, Bair W, Movshon JA. 2002a. Nature and interaction of signals from the receptive field center and surround in macaque V1 neurons. *J. Neurophysiol.* 88:2530–46

Cavanaugh JR, Bair W, Movshon JA. 2002b. Selectivity and spatial distribution of signals from the receptive field surround in macaque V1 neurons. *J. Neurophysiol.* 88:2547–56

Cavanaugh J, Monosov IE, McAlonan K, Berman R, Smith MK, et al. 2012. Optogenetic inactivation modifies monkey visuomotor behavior. *Neuron* 76:901–7

Chalupa LM, Williams RW, Hughes MJ. 1983. Visual response properties in the tectorecipient zone of the cat's lateral posterior-pulvinar complex: a comparison with the superior colliculus. *J. Neurosci.* 3:2587–96

Chariker L, Shapley R, Young L. 2016. Orientation selectivity from very sparse LGN inputs in a comprehensive model of macaque V1 cortex. *J. Neurosci.* 36:12368–84

Chen C, Kasamatsu T, Polat U, Norcia AM. 2001. Contrast response characteristics of long-range lateral interactions in cat striate cortex. *NeuroReport* 12:655–61

Chisum HJ, Mooser F, Fitzpatrick D. 2003. Emergent properties of layer 2/3 neurons reflect the collinear arrangement of horizontal connections in tree shrew visual cortex. *J. Neurosci.* 23:2947–60

Coen-Cagli R, Dayan P, Schwartz O. 2012. Cortical surround interactions and perceptual salience via natural scene statistics. *PLOS Comput. Biol.* 8:e1002405

Dantzker JL, Callaway EM. 2000. Laminar sources of synaptic input to cortical inhibitory interneurons and pyramidal neurons. *Nat. Neurosci.* 3:701–7

DeAngelis GC, Freeman RD, Ohzawa I. 1994. Length and width tuning of neurons in the cat's primary visual cortex. *J. Neurophysiol.* 71:347–74

Denman DJ, Contreras D. 2014. The structure of pairwise correlation in mouse primary visual cortex reveals functional organization in the absence of an orientation map. *Cereb. Cortex* 24:2707–20

Desimone R, Schein SJ. 1987. Visual properties of neurons in area V4 of the macaque: sensitivity to stimulus form. *J. Neurophysiol.* 57:835–68

Dimidschstein J, Chen Q, Tremblay R, Rogers SL, Saldi GA, et al. 2016. A viral strategy for targeting and manipulating interneurons across vertebrate species. *Nat. Neurosci.* 19:1743–49

El-Boustani S, Sur M. 2014. Response-dependent dynamics of cell-specific inhibition in cortical networks in vivo. *Nat. Commun.* 5:5689

Federer F, Merlin S, Angelucci A. 2015. Anatomical and functional specificity of V2-to-V1 feedback circuits in the primate visual cortex. Presented at Soc. Neurosci., Chicago, Abstr. 699.02

Field DJ. 1987. Relations between the statistics of natural images and the response properties of cortical cells. *J. Opt. Soc. Am. A* 4:2379–94

Field DJ, Golden JR, Hayes A. 2013. Contour integration and the association field. In *The New Visual Neurosciences*, ed. LM Chalupa, JS Werner, pp. 627–38. Cambridge, MA: MIT Press

Fino E, Yuste R. 2011. Dense inhibitory connectivity in neocortex. *Neuron* 69:1188–203

Galletti C, Gamberini M, Kutz DF, Fattori P, Luppino G, Matelli M. 2001. The cortical connections of area V6: an occipito-parietal network processing visual information. *Eur. J. Neurosci.* 13:1572–88

Geisler WS, Perry JS, Super BJ, Gallogly DP. 2001. Edge co-occurrence in natural images predicts contour grouping performance. *Vis. Res.* 41:711–24

Gerits A, Farivar R, Rosen BR, Wald LL, Boyden ES, Vanduffel W. 2012. Optogenetically induced behavioral and functional network changes in primates. *Curr. Biol.* 22:1722–26

Gilbert CD. 1977. Laminar differences in receptive field properties of cells in cat primary visual cortex. *J. Physiol.* 268:391–421

Gilbert CD, Wiesel TN. 1983. Clustered intrinsic connections in cat visual cortex. *J. Neurosci.* 3:1116–33

Gilbert CD, Wiesel TN. 1989. Columnar specificity of intrinsic horizontal and corticocortical connections in cat visual cortex. *J. Neurosci.* 9:2432–42

Girard P, Hupé JM, Bullier J. 2001. Feedforward and feedback connections between Areas V1 and V2 of the monkey have similar rapid conduction velocities. *J. Neurophysiol.* 85:1328–31

Goldberg ME, Wurtz RH. 1972. Activity of superior colliculus in behaving monkey. I. Visual receptive fields of single neurons. *J. Neurophysiol.* 35:542–59

Gonchar Y, Burkhalter A. 2003. Distinct GABAergic targets of feedforward and feedback connections between lower and higher areas of rat visual cortex. *J. Neurosci.* 23:10904–12

Grinvald A, Lieke EE, Frostig RD, Hildesheim R. 1994. Cortical point-spread function and long-range lateral interactions revealed by real-time optical imaging of macaque monkey primary visual cortex. *J. Neurosci.* 14:2545–68

Haider B, Krause MR, Duque A, Yu Y, Touryan J, et al. 2010. Synaptic and network mechanisms of sparse and reliable visual cortical activity during nonclassical receptive field stimulation. *Neuron* 65:107–21

Hashemi-Nezhad M, Lyon DC. 2012. Orientation tuning of the suppressive extraclassical surround depends on intrinsic organization of V1. *Cereb. Cortex* 22:308–26

Henry CA, Joshi S, Xing D, Shapley RM, Hawken MJ. 2013. Functional characterization of the extraclassical receptive field in macaque V1: contrast, orientation, and temporal dynamics. *J. Neurosci.* 33:6230–42

Hess R, Field D. 1999. Integration of contours: new insights. *Trends Cogn. Sci.* 3:480–86

Hofer SB, Ko H, Pichler B, Vogelstein J, Ros H, et al. 2011. Differential connectivity and response dynamics of excitatory and inhibitory neurons in visual cortex. *Nat. Neurosci.* 14:1045–52

Hubel DH, Wiesel TN. 1959. Receptive fields of single neurones in the cat's striate cortex. *J. Physiol.* 148:574–91

Hubel DH, Wiesel TN. 1962. Receptive fields, binocular interaction and functional architecture in the cat's visual cortex. *J. Physiol.* 160:106–54

Hubel DH, Wiesel TN. 1965. Receptive fields and functional architecture in two nonstriate visual areas (18 and 19) of the cat. *J. Neurophysiol.* 28:229–89

Hupé JM, James AC, Girard P, Bullier J. 2001. Response modulations by static texture surround in area V1 of the macaque monkey do not depend on feedback connections from V2. *J. Neurophysiol.* 85:146–63

Hupé JM, James AC, Payne BR, Lomber SG, Girard P, Bullier J. 1998. Cortical feedback improves discrimination between figure and background by V1, V2 and V3 neurons. *Nature* 394:784–87

Ichida JM, Schwabe L, Bressloff PC, Angelucci A. 2007. Response facilitation from the "suppressive" receptive field surround of macaque V1 neurons. *J. Neurophysiol.* 98:2168–81

Isaacson JS, Scanziani M. 2011. How inhibition shapes cortical activity. *Neuron* 72:231–43

Ito M, Gilbert CD. 1999. Attention modulates contextual influences in the primary visual cortex of alert monkeys. *Neuron* 22:593–604

Jiang X, Shen S, Cadwell CR, Berens P, Sinz F, et al. 2015. Principles of connectivity among morphologically defined cell types in adult neocortex. *Science* 350:aac9462

Kapadia MK, Ito M, Gilbert CD, Westheimer G. 1995. Improvement in visual sensitivity by changes in local context: parallel studies in human observers and in V1 of alert monkeys. *Neuron* 15:843–56

Kapfer C, Glickfeld LL, Atallah BV, Scanziani M. 2007. Supralinear increase of recurrent inhibition during sparse activity in the somatosensory cortex. *Nat. Neurosci.* 10:743–53

Kawaguchi Y, Kubota Y. 1997. GABAergic cell subtypes and their synaptic connections in rat frontal cortex. *Cereb. Cortex* 7:476–86

Kennedy H, Bullier J. 1985. A double-labeling investigation of the afferent connectivity to cortical area V1 and V2 of the macaque monkey. *J. Neurosci.* 5:2815–30

Kilpelainen M, Donner K, Laurinen P. 2007. Time course of suppression by surround gratings: highly contrast-dependent, but consistently fast. *Vis. Res.* 47:3298–306

Kisvárday ZF, Martin KAC, Freund TF, Maglóczky Z, Whitteridge D, Somogyi P. 1986. Synaptic targets of HRP-filled layer III pyramidal cells in the cat striate cortex. *Exp. Brain Res.* 64:541–52

Knierim JJ, Van Essen D. 1992. Neuronal responses to static texture patterns in area V1 of the alert macaque monkey. *J. Neurophysiol.* 67:961–80

Knudsen EI, Konishi M. 1978. Center-surround organization of auditory receptive fields in the owl. *Science* 202:778–80

Ko H, Hofer SB, Pichler B, Buchanan KA, Sjöström PJ, Mrsic-Flogel TD. 2011. Functional specificity of local synaptic connections in neocortical networks. *Nature* 473:87–91

Lamme VAF. 1995. The neurophysiology of figure-ground segregation in primary visual cortex. *J. Neurosci.* 15:1605–15

Lee SH, Kwan AC, Dan Y. 2014. Interneuron subtypes and orientation tuning. *Nature* 508:E1–2

Lee SH, Kwan AC, Zhang S, Phoumthipphavong V, Flannery JG, et al. 2012. Activation of specific interneurons improves V1 feature selectivity and visual perception. *Nature* 488:379–83

Levick WR, Cleland BG, Dubin MW. 1972. Lateral geniculate neurons of the cat: retinal inputs and physiology. *Investig. Ophthalm.* 11:302–11

Levitt JB, Lund JS. 1997. Contrast dependence of contextual effects in primate visual cortex. *Nature* 387:73–76

Levitt JB, Lund JS. 2002. The spatial extent over which neurons in macaque striate cortex pool visual signals. *Vis. Neurosci.* 19:439–52

Li C, Li W. 1994. Extensive integration field beyond the classical receptive field of cat's striate cortical neurons: classification and tuning properties. *Vision Res.* 34:2337–55

Lien AD, Scanziani M. 2013. Tuned thalamic excitation is amplified by visual cortical circuits. *Nat. Neurosci.* 16:1315–23

Lund JS, Wu Q, Hadingham PT, Levitt JB. 1995. Cells and circuits contributing to functional properties in area V1 of macaque monkey cerebral cortex: bases for neuroanatomically realistic models. *J. Anat.* 187:563–81

Ma WP, Liu BH, Li YT, Huang ZJ, Zhang LI, Tao HW. 2010. Visual representations by cortical somatostatin inhibitory neurons—selective but with weak and delayed responses. *J. Neurosci.* 30:14371–79

Ma Y, Hu H, Berrebi AS, Mathers PH, Agmon A. 2006. Distinct subtypes of somatostatin-containing neocortical interneurons revealed in transgenic mice. *J. Neurosci.* 26:5069–82

Maffei L, Fiorentini L. 1976. The unresponsive regions of visual cortical receptive fields. *Vis. Res.* 16:1131–39

Malach R, Amir Y, Harel M, Grinvald A. 1993. Relationship between intrinsic connections and functional architecture revealed by optical imaging and in vivo targeted biocytin injections in primate striate cortex. *PNAS* 90:10469–73

Marino J, Schummers J, Lyon DC, Schwabe L, Beck O, et al. 2005. Invariant computations in local cortical networks with balanced excitation and inhibition. *Nat. Neurosci.* 8:194–201

Marrocco RT, McClurkin JW, Young RA. 1982. Modulation of lateral geniculate nucleus cell responsiveness by visual activation of the corticogeniculate pathway. *J. Neurosci.* 2:256–63

Marshel JH, Kaye AP, Nauhaus I, Callaway EM. 2012. Anterior-posterior direction opponency in the superficial mouse lateral geniculate nucleus. *Neuron* 76:713–20

Maunsell JHR, Van Essen DC. 1983. The connections of the middle temporal visual area (MT) and their relationship to a cortical hierarchy in the macaque monkey. *J. Neurosci.* 3:2563–86

McAdams CJ, Reid CR. 2005. Attention modulates the responses of simple cells in monkey primary visual cortex. *J. Neurosci.* 25:11023–33

McGuire BA, Gilbert CD, Rivlin PK, Wiesel TN. 1991. Targets of horizontal connections in macaque primary visual cortex. *J. Comp. Neurol.* 305:370–92

McIlwain JT. 1964. Receptive fields of optic tract axons and lateral geniculate cells: peripheral extent and barbiturate sensitivity. *J. Neurophysiol.* 27:1154–73

Miller KD. 2016. Canonical computations of the cerebral cortex. *Curr. Opin. Neurobiol.* 37:75–84

Mitzdorf U. 1985. Current source-density method and application in cat cerebral cortex: investigation of evoked potentials and EEG phenomena. *Physiol. Rev.* 65:37–100

Müller JR, Metha AB, Krauskopf J, Lennie P. 2003. Local signals from beyond the receptive fields of striate cortical neurons. *J. Neurophysiol.* 90:822–31

Nassi JJ, Cepko CL, Born RT, Beier KT. 2015. Neuroanatomy goes viral! *Front. Neuroanat.* 9:80

Nassi JJ, Lomber SG, Born RT. 2013. Corticocortical feedback contributes to surround suppression in V1 of the alert primate. *J. Neurosci.* 33:8504–17

Nelson JI, Frost B. 1978. Orientation selective inhibition from beyond the classical visual receptive field. *Brain Res.* 139:359–65

Nienborg H, Hasenstaub A, Nauhaus I, Taniguchi H, Huang ZJ, Callaway EM. 2013. Contrast dependence and differential contributions from somatostatin- and parvalbumin-expressing neurons to spatial integration in mouse V1. *J. Neurosci.* 33:11145–54

Nothdurft HC, Gallant JL, Van Essen DC. 2000. Response profiles to texture border patterns in area V1. *Vis. Neurosci.* 17:421–36

Nurminen L, Angelucci A. 2014. Multiple components of surround modulation in primary visual cortex: multiple neural circuits with multiple functions? *Vis. Res.* 104:47–56

Nurminen L, Merlin S, Bijanzadeh M, Federer F, Angelucci A. 2016. Topdown feedback controls spatial summation and response gain in primate visual cortex. bioRvix 094680. **https://doi.org/10.1101/094680**

Okano H, Hikishima K, Iriki A, Sasaki E. 2012. The common marmoset as a novel animal model system for biomedical and neuroscience research applications. *Sem. Fetal Neonatal Med.* 17(6):336–40

Olsen SR, Wilson RI. 2008. Lateral presynaptic inhibition mediates gain control in an olfactory circuit. *Nature* 452:956–60

Olshausen BA, Field DJ. 1996. Emergence of simple-cell receptive field properties by learning a sparse code for natural images. *Nature* 381:607–9

Olshausen BA, Field DJ. 2004. Sparse coding of sensory inputs. *Curr. Opin. Neurobiol.* 14:481–87

Ozeki H, Finn IM, Schaffer ES, Miller KD, Ferster D. 2009. Inhibitory stabilization of the cortical network underlies visual surround suppression. *Neuron* 62:578–92

Ozeki H, Sadakane O, Akasaki T, Naito T, Shimegi S, Sato H. 2004. Relationship between excitation and inhibition underlying size tuning and contextual response modulation in the cat primary visual cortex. *J. Neurosci.* 24:1428–38

Pecka M, Han Y, Sader E, Mrsic-Flogel TD. 2014. Experience-dependent specialization of receptive field surround for selective coding of natural scenes. *Neuron* 84:457–69

Perkel DJ, Bullier J, Kennedy H. 1986. Topography of the afferent connectivity of area 17 in the macaque monkey: a double-labelling study. *J. Comp. Neurol.* 253:374–402

Petreanu L, Mao T, Sternson SM, Svoboda K. 2009. The subcellular organization of neocortical excitatory connections. *Nature* 457:1142–45

Petrov Y, McKee SP. 2006. The effect of spatial configuration on surround suppression of contrast sensitivity. *J. Vis.* 6:224–38

Pfeffer CK, Xue M, He M, Huang ZJ, Scanziani M. 2013. Inhibition of inhibition in visual cortex: the logic of connections between molecularly distinct interneurons. *Nat. Neurosci.* 16:1068–76

Phillips EA, Hasenstaub AR. 2016. Asymmetric effects of activating and inactivating cortical interneurons. *eLife* 5:e18383

Piscopo DM, El-Danaf RN, Huberman AD, Niell CM. 2013. Diverse visual features encoded in mouse lateral geniculate nucleus. *J. Neurosci.* 33:4642–56

Polat U, Mizobe K, Pettet MW, Kasamatsu T, Norcia AM. 1998. Collinear stimuli regulate visual responses depending on cell's contrast threshold. *Nature* 391:580–84

Priebe NJ, Ferster D. 2008. Inhibition, spike threshold, and stimulus selectivity in primary visual cortex. *Neuron* 57:482–97

Reid RC, Alonso JM. 1995. Specificity of monosynaptic connections from thalamus to visual cortex. *Nature* 378:281–84

Reyes A, Lujan R, Rozov A, Burnashev N, Somogyi P, Sakmann B. 1998. Target-cell-specific facilitation and depression in neocortical circuits. *Nat. Neurosci.* 1:279–85

Roberts MJ, Delicato LS, Herrero J, Gieselmann MA, Thiele A. 2007. Attention alters spatial integration in macaque V1 in an eccentricity dependent manner. *Nat. Neurosci.* 10:1483–91

Rockland KS. 1994. The organization of feedback connections from area V2 (18) to V1 (17). In *Primary Visual Cortex in Primates*, ed. A Peters, KS Rockland, pp. 261–99. New York: Plenum Press

Rockland KS, Knutson T. 2000. Feedback connections from area MT of the squirrel monkey to areas V1 and V2. *J. Comp. Neurol.* 425:345–68

Rockland KS, Lund JS. 1982. Widespread periodic intrinsic connections in the tree shrew visual cortex. *Science* 215:1532–34

Rockland KS, Lund JS. 1983. Intrinsic laminar lattice connections in primate visual cortex. *J. Comp. Neurol.* 216:303–18

Rockland KS, Pandya DN. 1979. Laminar origins and terminations of cortical connections of the occcipital lobe in the rhesus monkey. *Brain Res.* 179:3–20

Rockland KS, Virga A. 1989. Terminal arbors of individual "Feedback" axons projecting from area V2 to V1 in the macaque monkey: a study using immunohistochemistry of anterogradely transported *Phaseolus vulgaris*-leucoagglutinin. *J. Comp. Neurol.* 285:54–72

Rubin DB, Van Hooser SD, Miller KD. 2015. The stabilized supralinear network: a unifying circuit motif underlying multi-input integration in sensory cortex. *Neuron* 85:402–17

Sachdev RN, Krause MR, Mazer JA. 2012. Surround suppression and sparse coding in visual and barrel cortices. *Front. Neur. Circuits* 6:43

Sadakane O, Ozeki H, Naito T, Akasaki T, Kasamatsu T, Sato H. 2006. Contrast-dependent, contextual response modulation in primary visual cortex and lateral geniculate nucleus of the cat. *Eur. J. Neurosci.* 23:1633–42

Sato TK, Haider B, Hausser M, Carandini M. 2016. An excitatory basis for divisive normalization in visual cortex. *Nat. Neurosci.* 19:568–70

Sato TK, Hausser M, Carandini M. 2014. Distal connectivity causes summation and division across mouse visual cortex. *Nat. Neurosci.* 17:30–32

Sceniak MP, Chatterjee S, Callaway EM. 2006. Visual spatial summation in macaque geniculocortical afferents. *J. Neurophysiol.* 96:3474–84

Sceniak MP, Hawken MJ, Shapley RM. 2001. Visual spatial characterization of macaque V1 neurons. *J. Neurophysiol.* 85:1873–87

Sceniak MP, Ringach DL, Hawken MJ, Shapley R. 1999. Contrast's effect on spatial summation by macaque V1 neurons. *Nat. Neurosci.* 2:733–39

Schmidt KE, Goebel R, Löwell S, Singer W. 1997. The perceptual grouping criterion of colinearity is reflected by anisotropies of connections in the primary visual cortex. *Eur. J. Neurosci.* 9:1083–89

Scholl B, Tan AY, Corey J, Priebe NJ. 2013. Emergence of orientation selectivity in the mammalian visual pathway. *J. Neurosci.* 33:10616–24

Schwabe L, Ichida JM, Shushruth S, Mangapathy P, Angelucci A. 2010. Contrast-dependence of surround suppression in macaque V1: experimental testing of a recurrent network model. *NeuroImage* 52:777–92

Schwabe L, Obermayer K, Angelucci A, Bressloff PC. 2006. The role of feedback in shaping the extra-classical receptive field of cortical neurons: a recurrent network model. *J. Neurosci.* 26:9117–29

Schwartz O, Simoncelli EP. 2001. Natural signal statistics and sensory gain control. *Nat. Neurosci.* 4:819–25

Self MW, Lorteije JA, Vangeneugden J, van Beest EH, Grigore ME, et al. 2014. Orientation-tuned surround suppression in mouse visual cortex. *J. Neurosci.* 34:9290–304

Sengpiel F, Sen A, Blakemore C. 1997. Characteristics of surround inhibition in cat area 17. *Exp. Brain Res.* 116:216–28

Seybold BA, Phillips EA, Schreiner CE, Hasenstaub AR. 2015. Inhibitory actions unified by network integration. *Neuron* 87:1181–92

Shmuel A, Korman M, Sterkin A, Harel M, Ullman S, et al. 2005. Retinotopic axis specificity and selective clustering of feedback projections from V2 to V1 in the owl monkey. *J. Neurosci.* 25:2117–31

Shushruth S, Ichida JM, Levitt JB, Angelucci A. 2009. Comparison of spatial summation properties of neurons in macaque V1 and V2. *J. Neurophysiol.* 102:2069–83

Shushruth S, Mangapathy P, Ichida JM, Bressloff PC, Schwabe L, Angelucci A. 2012. Strong recurrent networks compute the orientation-tuning of surround modulation in primate primary visual cortex. *J. Neurosci.* 4:308–21

Shushruth S, Nurminen L, Bijanzadeh M, Ichida JM, Vanni S, Angelucci A. 2013. Different orientation-tuning of near and far surround suppression in macaque primary visual cortex mirrors their tuning in human perception. *J. Neurosci.* 33:106–19

Silberberg G, Markram H. 2007. Disynaptic inhibition between neocortical pyramidal cells mediated by Martinotti cells. *Neuron* 53:735–46

Sillito AM, Grieve KL, Jones HE, Cudeiro J, Davis J. 1995. Visual cortical mechanisms detecting focal orientation discontinuities. *Nature* 378:492–96

Sincich LC, Blasdel GG. 2001. Oriented axon projections in primary visual cortex of the monkey. *J. Neurosci.* 21:4416–26

Slovin H, Arieli A, Hildesheim R, Grinvald A. 2002. Long-term voltage-sensitive dye imaging reveals cortical dynamics in behaving monkeys. *J. Neurophysiol.* 88:3421–38

Solomon SG, Lee BB, Sun H. 2006. Suppressive surrounds and contrast gain in magnocellular-pathway retinal ganglion cells of macaque. *J. Neurosci.* 26:8715–26

Solomon SG, White AJR, Martin PR. 2002. Extra-classical receptive field properties of parvocellular, magnocellular, and koniocellular cells in the primate lateral geniculate nucleus. *J. Neurosci.* 22:338–49

Somers DC, Todorov EV, Siapas AG, Toth LJ, Kim DS, Sur M. 1998. A local circuit approach to understanding integration of long-range inputs in primary visual cortex. *Cereb. Cortex* 8:204–17
Song XM, Li CY. 2008. Contrast-dependent and contrast-independent spatial summation of primary visual cortical neurons of the cat. *Cereb. Cortex* 18:331–36
Sterling P, Wickelgren BG. 1969. Visual receptive fields in the superior colliculus of the cat. *J. Neurophysiol.* 32:1–15
Stettler DD, Das A, Bennett J, Gilbert CD. 2002. Lateral connectivity and contextual interactions in macaque primary visual cortex. *Neuron* 36:739–50
Stimberg M, Wimmer K, Martin R, Schwabe L, Marino J, et al. 2009. The operating regime of local computations in primary visual cortex. *Cereb. Cortex* 19:2166–80
Sutter ML, Schreiner CE, McLean M, O'Connor KN, Loftus WC. 1999. Organization of inhibitory frequency receptive fields in cat primary auditory cortex. *J. Neurophysiol.* 82:2358–71
Tremblay R, Lee S, Rudy B. 2016. GABAergic interneurons in the neocortex: from cellular properties to circuits. *Neuron* 91:260–92
Ts'o DY, Gilbert CD, Wiesel TN. 1986. Relationships between horizontal interactions and functional architecture in cat striate cortex as revealed by cross-correlation analysis. *J. Neurosci.* 6:1160–70
Van den Bergh G, Zhang B, Arckens L, Chino YM. 2010. Receptive-field properties of V1 and V2 neurons in mice and macaque monkeys. *J. Comp. Neurol.* 518:2051–70
van Vreeswijk C, Sompolinsky H. 1996. Chaos in neuronal networks with balanced excitatory and inhibitory activity. *Science* 274:1724–26
Vanni S, Rosenström T. 2011. Local non-linear interactions in the visual cortex may reflect global decorrelation. *J. Comput. Neurosci.* 30:109–24
Vega-Bermudez F, Johnson KO. 1999. Surround suppression in the responses of primate SA1 and RA mechanoreceptive afferents mapped with a probe array. *J. Neurophysiol.* 81:2711–19
Vinje WE, Gallant JL. 2000. Sparse coding and decorrelation in primary visual cortex during natural vision. *Science* 287:1273–76
Vinje WE, Gallant JL. 2002. Natural stimulation of the nonclassical receptive field increase information transmission efficiency in V1. *J. Neurosci.* 22:2904–15
Walker GA, Ohzawa I, Freeman RD. 1999. Asymmetric suppression outside the classical receptive field of the visual cortex. *J. Neurosci.* 19:10536–53
Walker GA, Ohzawa I, Freeman RD. 2000. Suppression outside the classical cortical receptive field. *Vis. Neurosci.* 17:369–79
Wang C, Huang JY, Bardy C, FitzGibbon T, Dreher B. 2010. Influence of 'feedback' signals on spatial integration in receptive fields of cat area 17 neurons. *Brain Res.* 1328:34–48
Webb BS, Dhruv NT, Solomon SG, Taliby C, Lennie P. 2005. Early and late mechanisms of surround suppression in striate cortex of macaque. *J. Neurosci.* 25:11666–75
Webb BS, Tinsley CJ, Barraclough NE, Easton A, Parker A, Derrington AM. 2002. Feedback from V1 and inhibition from beyond the classical receptive field modulates the responses of neurons in the primate lateral geniculate nucleus. *Vis. Neurosci.* 19:583–92
Wilson NR, Runyan CA, Wang FL, Sur M. 2012. Division and subtraction by distinct cortical inhibitory networks in vivo. *Nature* 488:343–48
Wilson DE, Smith GB, Jacob AL, Walker T, Dimidschstein J, et al. 2017. GABAergic neurons in ferret visual cortex participate in functionally specialized networks. *Neuron* 93:1058–65
Wolf F, Engelken R, Puelma-Touzel M, Weidinger JDF, Neef A. 2014. Dynamical models of cortical circuits. *Curr. Opin. Neurobiol.* 25:228–36
Xu H, Jeong HY, Tremblay R, Rudy B. 2013. Neocortical somatostatin-expressing GABAergic interneurons disinhibit the thalamorecipient layer 4. *Neuron* 77:155–67
Zhang F, Aravanis AM, Adamantidis A, de Lecea L, Deisseroth K. 2007. Circuit-breakers: optical technologies for probing neural signals and systems. *Nat. Rev. Neurosci.* 8:577–81
Zhang S, Xu M, Kamigaki T, Hoang Do JP, Chang WC, et al. 2014. Long-range and local circuits for top-down modulation of visual cortex processing. *Science* 345:660–65
Zhao X, Chen H, Liu X, Cang J. 2013. Orientation-selective responses in the mouse lateral geniculate nucleus. *J. Neurosci.* 33:12751–63